Article:
Rymaruk, M.J., O'Brien, C.T., Brown, S.L. et al. (2019) Effect of core cross-linking on the physical properties of poly(dimethylsiloxane)-based diblock copolymer worms prepared in silicone oil. Macromolecules, 52 (18). pp. 6849-6860. ISSN: 0024-9297

https://doi.org/10.1021/acs.macromol.9b01488

Effect of Core Crosslinking on the Physical Properties of Polydimethylsiloxane-based Diblock Copolymer Worms Prepared in Silicone Oil

Matthew J. Rymaruk,[a,*] *Cate T. O'Brien,*[a] *Steven L. Brown,*[b] *Clive N. Williams,*[b] *and Steven P. Armes*[a,*]

a. Dainton Building, Department of Chemistry, University of Sheffield, Brook Hill, Sheffield, South Yorkshire, S3 7HF, UK.

b. Scott Bader Company Ltd, Wollaston, Wellingborough, Northamptonshire, NN29 7RL, UK.

*Authors to whom correspondence should be addressed (s.p.armes@sheffield.ac.uk, m.rymaruk@sheffield.ac.uk).

For use as table of contents graphic

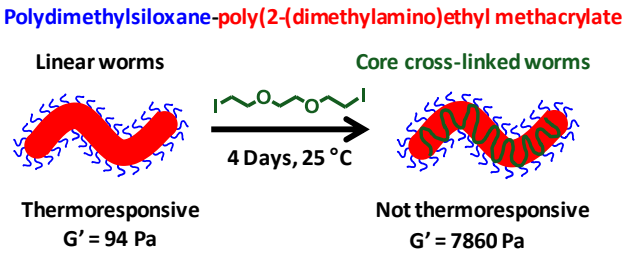

Abstract. A trithiocarbonate-capped polydimethylsiloxane (PDMS) precursor is chain-extended via reversible addition-fragmentation chain transfer (RAFT) dispersion polymerization of 2-(dimethylamino)ethyl methacrylate (DMA) in D5 silicone oil at 90 °C. For a fixed mean degree of polymerization (DP) of 66 for the PDMS steric stabilizer block, targeting core-forming PDMA block DPs of between 105 and 190 enables the preparation of either well-defined worms or vesicles at a copolymer concentration of 25% w/w. The as-synthesized linear $PDMS_{66}$-$PDMA_{100}$ worms exhibit thermoresponsive behavior in D5, undergoing a worm-to-sphere transition on heating to 100 °C. Variable temperature ^{1}H NMR spectroscopy indicates that this thermal transition is driven by reversible solvent plasticization of the PDMA cores. This change in copolymer morphology is characterized by TEM studies and variable temperature DLS, and SAXS experiments. Oscillatory rheology studies indicate that degelation occurs at 32 °C, but shear-induced polarized light imaging (SIPLI) measurements suggest that full conversion of worms into spheres requires significantly higher temperatures (~110 °C). 1,2-Bis(2-iodoethoxy)ethane (BIEE) is evaluated as a cross-linker for $PDMS_{66}$-$PDMA_x$ diblock copolymer nano-objects in D5. This bifunctional reagent quaternizes the tertiary amine groups on the DMA residues within the worm cores, introducing cross-links via the Menshutkin reaction. TEM studies confirm that such covalently-stabilized worms no longer undergo a worm-to-sphere transition when heated to 100 °C. Kinetic studies performed on $PDMS_{66}$-$PDMA_{176}$ vesicles suggest that crosslinking requires approximately 13 h at 20 °C to ensure that these nano-objects remain intact when dispersed in chloroform, which is a good solvent for both blocks. Oscillatory rheology studies of a $PDMS_{66}$-$PDMA_{100}$ worm gel indicated that covalent stabilization using a BIEE/DMA molar ratio of 0.15 increased its dynamic elastic modulus (G') by almost two orders of magnitude. Furthermore, such cross-linked worms exhibit a much lower critical gelation concentration (~2% w/w) compared to that of the linear precursor worms (~12% w/w).

INTRODUCTION

Over the past decade or so, the development of polymerization-induced self-assembly (PISA) has enabled the synthesis of well-defined diblock copolymer nanoparticles at copolymer concentrations of up to 50 % w/w.[1–4] This approach addresses the inherent problems associated with block copolymer self-assembly, which typically involves dilute copolymer solutions and one or more post-polymerization processing steps.[5] PISA syntheses are highly reproducible and the construction of phase diagrams ensures the reliable targeting of pure spheres, worms or vesicles under optimized conditions.[6,7] Recently, considerable attention has been paid to exploring potential applications for block copolymer nanoparticles prepared via PISA. For example, Mable *et al*. reported that poly(glycerol monomethacrylate)-poly(2-hydroxypropyl methacrylate) (PGMA-PHPMA) vesicles can be used for the encapsulation and controlled release of model payloads, e.g. silica nanoparticles or globular proteins such as bovine serum albumin (BSA).[8] Similarly, Canton *et al*. demonstrated that PGMA-PHPMA worms can be used as a long-term storage medium for colonies of human pluripotent stem cells.[9] More recently, PHPMA-based framboidal triblock copolymer vesicles have been exploited to selectively target triple-negative breast cancer cells.[10] Finally, various examples of spheres, worms and vesicles have been evaluated as bespoke Pickering emulsifiers of tunable surface wettability.[11–16]

In recent years, there have been various reports of the chemical modification of diblock copolymer nanoparticles to enhance their structural integrity. For example, nanoparticle crosslinking can be achieved by either (i) core cross-linking[17] or (ii) shell cross-linking.[18] Shell cross-linked micelles are produced by cross-linking the corona layer.[19–31] However, such covalent stabilization is usually limited to rather low copolymer concentrations (typically less than 1% w/w) for diblock copolymer micelles, otherwise inter-

particle cross-linking occurs. In contrast, core cross-linking usually avoids the problem of inter-particle cross-linking, because the reaction is confined within the micelle interior.[32–34] This concept was first demonstrated almost forty years ago, when UV radiation was utilized to crosslink polybutadiene-core spherical micelles in non-aqueous media.[35] A similar approach was adopted by both Antonietti and co-workers and Bates and co-workers to crosslink poly(ethylene oxide)-polybutadiene (PEO-PB) block copolymer nano-objects in water. In the former case, γ-rays were used to crosslink the pendent vinyl groups present on the core-forming block,[36] whereas free radical chemistry was utilized in the latter case.[37]

Various strategies have been explored for the production of core cross-linked micelles prepared via PISA. Perhaps the most common approach involves the copolymerization of a small quantity of a bifunctional monomer such as ethylene glycol dimethacrylate (EGDMA) towards the end of the PISA synthesis.[12,38–40] This works well for both spherical micelles and vesicles, because such copolymer morphologies occupy relatively broad phase space. As such, the subtle change in diblock composition owing to the introduction of a cross-linking comonomer does not normally lead to any change in morphology. However, worms typically occupy rather narrow phase space,[41] so attempts to conduct core cross-linking in this case often leads to the formation of mixed phases.[12] In principle, this problem can be avoided if the core-forming block contains appropriate functionality to enable cross-linking via post-polymerization modification using a suitable reagent. This concept was demonstrated by Liu *et al.*, who used UV irradiation to covalently stabilize cinnamoyl-functionalized AB diblock copolymer worms but this prior study did not involve PISA-synthesized nanoparticles.[42] In the context of PISA, Lovett *et al.*[41] statistically copolymerized HPMA with glycidyl methacrylate (GlyMA) to prepare linear PGMA-P(HPMA-stat-GlyMA) diblock copolymer worms with epoxy-functional cores. Addition of 3-aminopropyltriethoxysilane to aqueous

dispersions of such worms led to ring-opening of the epoxide groups on the GlyMA residues via epoxy-amine chemistry. Concomitant core cross-linking occurred via hydrolysis/condensation reactions between the pendent trialkoxysilane groups and the secondary hydroxyl groups on the HPMA residues. Similarly, Penfold *et al.*[43] found that the 3-aminopropyltriethoxysilane cross-linker could be replaced by 3-mercaptopropyl siloxane, with the latter reagent ensuring that no cationic charge was introduced into the worm cores. A different strategy was utilized by Byard *et al*., who prepared diblock copolymer spheres, worms or vesicles comprising poly(diacetone acrylamide) (PDAAM) cores.[44] In this case, addition of adipic acid dihydrazide to aqueous dispersions of such nano-objects resulted in cross-linking via hydrazone bond formation.[45] Similarly, Armes and co-workers used various diamines to cross-link PGlyMA-core spheres prepared via RAFT polymerization in either water[46] or mineral oil.[47]

Recently, we reported the PISA synthesis of linear polydimethylsiloxane-poly(2-(dimethylamino)ethyl methacrylate) [PDMS-PDMA] diblock copolymer nano-objects in a low-viscosity silicone oil (decamethylcyclopentasiloxane or D5),[48] see **Figure 1a**. Systematically increasing the degree of polymerization (DP) of the PDMA block enabled the reproducible synthesis of spheres, worms or vesicles at 25% w/w solids. This is a rather rare example of a PISA formulation in which a tertiary amine methacrylate (i.e. DMA) is used for the structure-directing block.[49] Bütün and co-workers reported that PDMA-based spherical micelles could be cross-linked via the Menshutkin reaction[50] utilizing 1,2-bis(2-iodoethoxy)ethane (BIEE) in either water or *n*-hexane.[26,28,29] In the present study, the feasibility of using the same bifunctional reagent to prepare covalently-stabilized $PDMS_{66}$-$PDMA_x$ nano-objects directly in silicone oil is explored (see **Figure 1a**). Particular attention is paid to the synthesis of core cross-linked worms, and the effect of such covalent

stabilization on their gel strength, critical gelation concentration (CGC) and thermoresponsive behavior (see **Figure 1b**). This is because such highly anisotropic nanoparticles are expected to be potentially useful thickeners for silicones.[48]

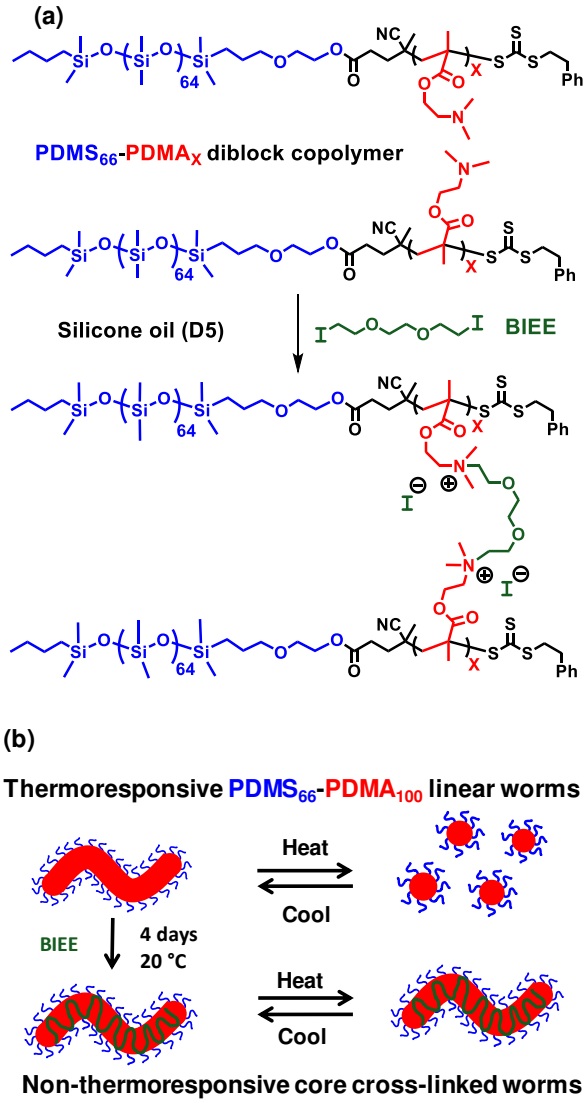

Figure 1. (a) Chemical structure of a $PDMS_{66}$-$PDMA_x$ diblock copolymer and the crosslinking of its DMA residues within worm cores via the Menshutkin reaction using 1,2-bis(iodoethoxy)ethane (BIEE). (b) Schematic representation of the thermoresponsive behavior of linear $PDMS_{66}$-$PDMA_{100}$ worms prepared directly in D5 silicone oil via PISA, which undergo a worm-to-sphere transition on heating. In contrast, the analogous core cross-linked worms prepared using BIEE exhibit no thermoresponsive behavior under the same conditions.

EXPERIMENTAL SECTION

Materials. Monocarbinol-terminated PDMS (M_n = 5 000 g mol^{-1}, mean DP = 66) was purchased from Fluorochem (Hadfield, UK) and used as received. D5 was provided by the Scott Bader Company Ltd (Wollaston, UK). Trigonox 21s (T21s) initiator was purchased from AkzoNobel (Amersfoort, The Netherlands). DMA, BIEE, triethylamine (TEA), butylated hydroxytoluene (BHT), *N,N'*dicyclohexylcarbodiimide (DCC), 4-dimethylaminopyridine (DMAP), dichloromethane (DCM), tetrahydrofuran (THF), pyridine, chloroform and trimethylamine (TEA) were purchased from Sigma Aldrich (Dorset, UK). Toluene-d_8, dichloromethane-d_2, and chloroform-d were obtained from Goss Scientific (Crewe, UK). 4-Cyano-4-(2-phenylethanesulfanylthiocarbonyl)sulfanylpentanoic acid (PETTC) was synthesized according to a literature protocol.[11] DMA was passed through basic alumina prior to use to remove its inhibitor. All other reagents were used as received unless otherwise stated.

Methods

Synthesis of $PDMS_{66}$ macro-CTA.

A $PDMS_{66}$-trithiocarbonate macro-CTA ($PDMS_{66}$-TTC) was synthesized according to a previously reported protocol.[48]

Synthesis of $PDMS_{66}$-$PDMA_x$ diblock copolymer nano-objects in D5 silicone oil

$PDMS_{66}$-$PDMA_x$ nano-objects were synthesized in D5 silicone oil at 25% w/w solids according to a previously described protocol.[48] Pure worms or vesicles were obtained when targeting x = 100 or 176 for the PDMA block, respectively. Characterization data for these two copolymers are summarized in **Table S1**. A typical protocol for the PISA synthesis of $PDMS_{66}$-$PDMA_{100}$ is as follows: The trithiocarbonate-based $PDMS_{66}$-TTC precursor (0.20 g,

37.6 μmol) was added to a 10 ml reaction vial. Then D5 silicone oil (1.85 g) and DMA (0.62 g, 3.95 mmol) were added to target a PDMA DP of 105 at 25% w/w solids. Next, T21s initiator was added (30 μl of a 10% v/v solution in D5; 2.7 mg, 12.5 μmol) and the reaction mixture was purged with nitrogen gas at 20 °C for 20 min. Then the reaction vial was placed in a pre-heated oil bath set at 90 °C for 5 h. The resulting diblock copolymer dispersion was obtained as a free-flowing fluid at 90 °C and formed a free-standing gel on cooling to 20 °C. ^{1}H NMR spectroscopy studies in $CDCl_3$ indicated 95% DMA conversion and THF GPC analysis indicated M_n = 20,900 g mol^{-1} and M_w/M_n = 1.21.

Cross-linking protocol

A typical core cross-linking protocol was conducted as follows: a 25% w/w dispersion of $PDMS_{66}$-$PDMA_{100}$ worms (1.0 g, 12 μmol) in D5 was placed in a vial using a spatula. To this worm gel, BIEE was added (32.0 μl, 0.18 mmol) to target a BIEE/DMA molar ratio of 0.15 (i.e. 15 units of BIEE per $PDMS_{66}$-$PDMA_{100}$ copolymer chain). Gentle stirring with a spatula was then required to ensure full BIEE dissolution within the gel. The resulting dispersion was allowed to stand for 4 days at 20 °C to ensure that core cross-linking occurred. In a series of related experiments, the amount of added BIEE was systematically lowered to target BIEE/DMA molar ratios ranging from 0.05 to 0.15.

Characterization

Gel permeation chromatography

The THF GPC set-up comprised an Agilent Infinity series degasser and pump, two Agilent PLgel 5 μm Mixed C columns in series and a refractive index detector operating at 30 °C. The THF eluent contained trimethylamine (2.0 % w/w) and butylated hydroxytoluene (0.05 % w/v) and the flow rate was 1.0 ml min^{-1}. Calibration was achieved using twelve near-

monodisperse poly(methyl methacrylate) standards ranging from 800 g mol^{-1} up to 2,200,000 g mol^{-1}.

^{1}H NMR spectroscopy

Spectra were recorded at 20 °C in $CDCl_3$ using a Bruker Avance III HD 400 spectrometer operating at 400 MHz (typically averaging 64 scans per spectrum).

Variable temperature ^{1}H NMR spectroscopy

Variable temperature ^{1}H NMR experiments were performed using a Bruker Avance 111 HD spectrometer operating at 500 MHz. Samples were equilibrated for 15 min at each temperature prior to analysis, and 64 scans were averaged per spectrum.

Transmission electron microscopy

Transmission electron microscopy (TEM) studies were conducted using a FEI Tecnai G2 spirit instrument operating at 80 kV and equipped with a Gatan 1k CCD camera. Copper mesh TEM grids were coated in-house with a thin film of amorphous carbon. The carbon-coated grids were then loaded with a single droplet of a dilute copolymer dispersion (0.1% w/w). Prior to imaging, each TEM grid was exposed to ruthenium(IV) vapor for 7 min at 20 °C to enhance electron contrast. The ruthenium oxide stain was prepared by adding ruthenium(II) oxide (0.30 g) to water (50 g), to form a slurry. Then sodium periodate (2.0 g) was added to this stirred mixture and a yellow solution of ruthenium(IV) oxide was formed within 1 min.[51]

Dynamic light scattering

DLS studies were performed using a Zetasizer Nano-ZS instrument (Malvern Instruments, UK) at 25 °C at a fixed scattering angle of 173°. Typically, dispersions were diluted to 0.25%

w/w prior to analysis. The sphere-equivalent Z-average diameter and polydispersity (PDI) of the diblock copolymer nano-objects were calculated by cumulants analysis of the experimental correlation function using Dispersion Technology Software version 6.20. Data were averaged over ten runs with each run being of thirty seconds duration. A heating rate of 2 °C min^{-1} was used for variable temperature DLS measurements.

Determination of the critical gelation temperature (CGT) for linear and cross-linked $PDMS_{66}$-$PDMA_{100}$ worms. An AR-G2 rheometer equipped with a 40 mm 2° aluminum cone was used for all measurements. The storage and loss moduli (G' and G'', respectively) were determined by oscillatory rheometry as a function of temperature at an angular frequency of 1.0 rad s^{-1} and an applied strain of 1.0%. In all cases, the gap between the cone and plate was 56 μm, and the heating rate was 2 °C min^{-1}.

Determination of the critical gelation concentration (CGC) of cross-linked $PDMS_{66}$-$PDMA_{100}$ worms. An Anton Paar MCR 502 rheometer equipped with a cup (20 mL volume) and bob was utilized for all measurements. G' and G'' were analyzed as a function of angular frequency at an applied strain of 1%. In all cases, the sample gap was 2 mm and the temperature was 25 °C. Approximately 10 mL of copolymer dispersion was used per measurement, with copolymer concentrations ranging from 1 to 8% w/w.

Shear-induced polarized light imaging

Shear alignment experiments were conducted using a mechano-optical rheometer (an Anton Paar Physica MCR301 instrument equipped with a SIPLI accessory.[52,53] Measurements were performed using a plate−plate geometry comprising a 25 mm polished steel plate and a fused quartz plate connected to a variable temperature Peltier system. The gap between plates was

set at 0.5 mm for all experiments, the shear rate was fixed at 2.0 s^{-1} and a heating rate of 5 °C min^{-1} was utilized for all experiments. Sample illumination was achieved using an Edmund Optics 150 W MI-150 high-intensity fiber optic white light source. The polarizer and analyzer axes were crossed at 90° to obtain polarized light images, which were recorded using a color CCD camera (Lumenera Lu165c).

Small-angle X-ray scattering

SAXS patterns were recorded at a synchrotron source (ESRF, station ID02, Grenoble, France) using monochromatic X-ray radiation (wavelength λ = 0.0995 nm, with q ranging from 0.004 to 2.5 nm^{-1}, where q is the length of the scattering vector, i.e. $q = 4\pi \sin\theta/\lambda$ and θ is one-half of the scattering angle) and a Rayonix MX-170HS Kodak CCD detector. All measurements were conducted on 1.0% w/w dispersions. A heating rate of 30 °C min^{-1} was utilized for each experiment. X-ray scattering data were reduced and normalized using standard routines provided by the beamline facility.

RESULTS AND DISCUSSION

A trithiocarbonate-functionalized $PDMS_{66}$ precursor was prepared by esterification of a monocarbinol-terminated $PDMS_{66}$ using PETTC, DCC and DMAP according to a previously reported protocol.[48] ^{1}H NMR and UV spectroscopy studies indicated mean degrees of esterification of 92 ± 4 % and 94 ± 5 %, respectively. This precursor was then chain-extended with DMA at 25% w/w solids in D5, targeting a PDMA DP of either 105 or 190, which corresponded to either pure worms or vesicles respectively.[48] ^{1}H NMR spectroscopy studies in $CDCl_3$ indicated that DMA conversions of 95 % (worms) and 93 % (vesicles) were achieved within 5 h at 90°C. The resulting $PDMS_{66}$-$PDMA_{100}$ and $PDMS_{66}$-$PDMA_{176}$ worms and vesicles were further characterized by TEM and GPC, as summarized in **Table S1**.

The thermoresponsive nature of diblock copolymer nanoparticles prepared in various solvents *via* PISA is well-documented.[54–59] Typically, a morphological transition occurs as a result of surface plasticization of the core-forming block owing to solvent ingress on varying the temperature. Thus, the effective stabilizer volume fraction increases and either a worm-to-sphere[58] or a vesicle-to-worm[60] morphological transition is observed. For aqueous PISA formulations, the nanoparticle cores typically become more hydrated at lower temperature, which has been described as lower critical solution temperature (LCST)-like behavior.[61] Hence a worm-to-sphere transition can be observed on cooling in this case.[59] The opposite behavior is normally observed for diblock copolymer nano-objects prepared in non-aqueous media, since the core-forming block usually exhibits upper critical solution temperature (UCST)-like behavior under such conditions. Hence, a worm-to-sphere (or vesicle-to-worm) transition can be observed on heating.[58,60] To investigate whether $PDMS_{66}$-$PDMA_{100}$ worms prepared in D5 exhibited thermoresponsive behavior, a 25% w/w copolymer dispersion was heated up to 100 °C for 30 min (see **Figure 2**).

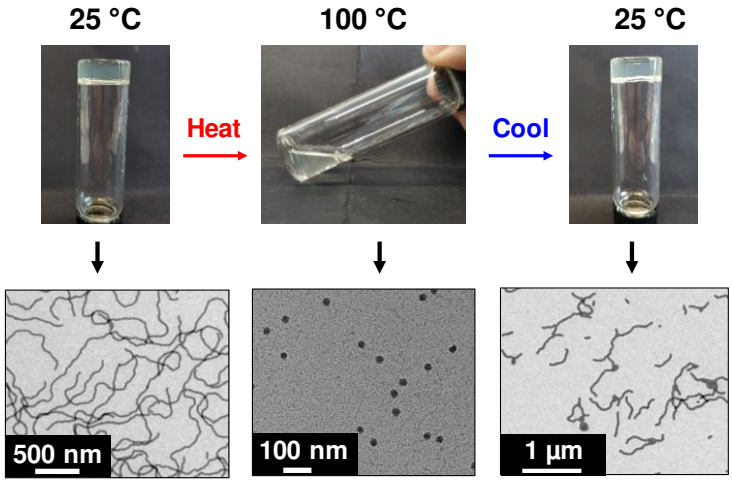

Figure 2. Reversible (de)gelation observed on heating a 25% w/w dispersion of a $PDMS_{66}$-$PDMA_{100}$ worm gel prepared in D5 silicone oil up to 100 °C for 30 min, followed by cooling to 25 °C. The corresponding TEM images indicate the initial worm morphology at 25 °C, the intermediate spherical morphology obtained at 100 °C and the reconstituted worm morphology formed at 25 °C.

This concentrated worm dispersion formed a soft free-standing gel at ambient temperature, most likely owing to multiple inter-worm contacts.[62] However, a free-flowing fluid was obtained at 100 °C. Moreover, this thermal transition proved to be reversible, with regelation being observed within 1 h on cooling to 25 °C. TEM studies performed on 0.1% w/w dispersions of $PDMS_{66}$-$PDMA_{100}$ worms confirmed that degelation was the result of a worm-to-sphere transition. The preparation of TEM grids to image the worms at 100 °C was conducted as follows. A small piece of a 25% w/w worm gel was first heated to 100 °C to induce degelation. The resulting free-flowing fluid was then diluted to 0.1% w/w using D5 solvent that had been preheated to 100 °C. In principle, dilution to such a low concentration should kinetically trap the spherical morphology formed at high temperature,[58] thus preventing the sphere-to-worm transition from occurring on cooling. In view of the relatively low T_g (~18 °C[63]) for the PDMA core-forming block, the resulting dilute dispersion was then cooled to approximately 3 °C when preparing the TEM grid in order to prevent film formation.

Variable temperature ^{1}H NMR studies were performed to further investigate this thermoresponsive behavior. Thus, a 5.0% w/w $PDMS_{66}$-$PDMA_{100}$ worm dispersion was heated from 20 °C to 100 °C, and the degree of solvation of the PDMA core-forming block was monitored relative to an external standard (pyridine) located within a coaxial inner NMR tube (**Figure 3a**). N.B. for clarity, the spectra are only shown between 2 ppm and 9 ppm. The $PDMS_{66}$ stabilizer signals are located below 2 ppm but they are obscured by the signals arising from 95 % w/w D5 solvent, which dominate the spectra at all temperatures. This is why an external standard was utilized in such experiments.

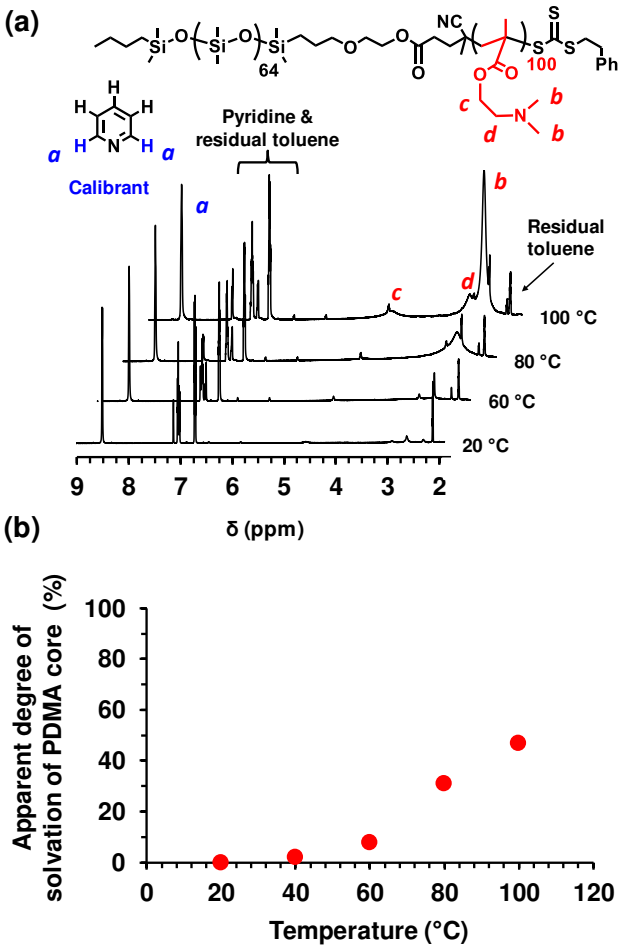

Figure 3. (a) ^{1}H NMR spectra recorded at various temperatures for a 5.0% w/w dispersion of $PDMS_{66}$-$PDMA_{100}$ worms in D5. The NMR tube was equipped with a coaxial inner tube containing toluene-d_8 as a lock solvent and 0.1 M pyridine as an external standard. (b) Apparent degree of solvation of the $PDMA_{100}$ core block as a function of temperature. The former parameter was calculated by integrating the signals assigned to the six equivalent dimethylamino protons and two azamethylene protons (labeled *b* and *d* respectively) of the PDMA core block relative to the signal assigned to the pyridine standard at 8.5 ppm (labeled *a*).

Above 40 °C, the integrated signals assigned to the six equivalent dimethylamino protons at 2.65 ppm and two neighboring azamethylene protons at around 2.93 ppm (labeled *b* and *d* respectively in **Figure 3a**) become significantly more intense relative to the integrated pyridine signal *a* observed at 8.5 ppm. This indicates that the PDMA core-forming block becomes increasingly plasticized by hot D5 solvent at elevated temperatures. Indeed, a mean

degree of solvation of up to 50% is observed at 100 °C, see **Figure 3b**. Moreover, this change in solvation is fully reversible, with subsequent attenuation of the PDMA core-forming block signals being observed on cooling to 20 °C (see **Figure S1**). Similar behavior was observed by Fielding *et al.* when heating poly(benzyl methacrylate)-core diblock copolymer worms in d_{26}-dodecane to produce spheres.[58] In both cases, surface plasticization of the worm cores by hot solvent drives the ensuing worm-to-sphere transition: such partial solvation effectively shifts the relative volume fractions of the core and stabilizer blocks such that spherical micelles become the thermodynamically-preferred copolymer morphology.

Twenty years ago, Armes and co-workers reported that BIEE could be used to prepare shell cross-linked micelles in aqueous solution.[26–28,50,64] This bifunctional reagent reacts with the pendent tertiary amine groups present in the corona-forming PDMA block via the Menshutkin reaction.[50] Although such quaternization undoubtedly leads to the formation of an unknown fraction of intra-chain loops, a sufficient number of inter-chain cross-links are formed to ensure covalent stabilization of the micelles. To examine whether the same strategy could be used to prepare core cross-linked worms, BIEE was added to a 25% w/w dispersion of a $PDMS_{66}$-$PDMA_{100}$ worm gel in D5 at 20 °C. In this initial scoping experiment, a BIEE/DMA molar ratio of 0.15 was utilized. The worm gel was stirred with a spatula to ensure intimate mixing with the BIEE and then allowed to stand at 20 °C for five days. In contrast to the original linear $PDMS_{66}$-$PDMA_{100}$ worms (see **Figure 2**), no degelation occurred when subsequently heating this BIEE-treated worm gel up to 100 °C, (**Figure 4a**), which indicated that no worm-to-sphere transition had occurred. This was confirmed by TEM studies, which indicated that the worms that are initially present at room temperature remained intact at 100 °C, suggesting successful core cross-linking (**Figure 4a**). This is

consistent with the PISA literature: for example, Busatto et al. reported similar behavior for covalently-stabilized worms prepared in ethanol.[65]

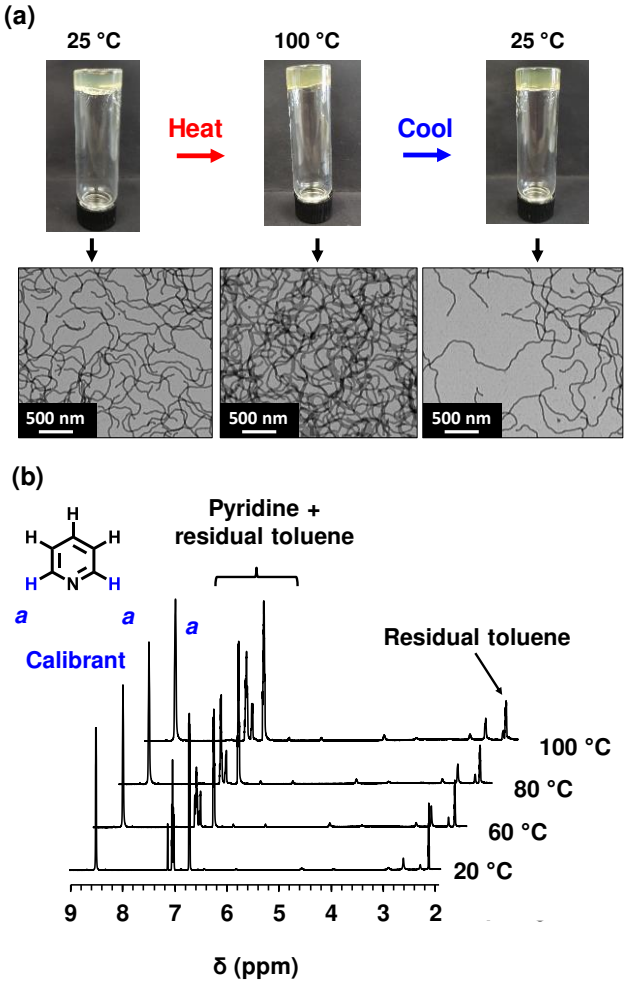

Figure 4. (a) Tube inversion tests indicate that no degelation occurred on heating a 25% w/w dispersion of cross-linked $PDMS_{66}$-$PDMA_{100}$ worms (prepared using a BIEE/DMA molar ratio of 0.15) in D5 silicone oil at 100 °C for 30 min, followed by cooling to 25 °C. The corresponding TEM images confirm that the original worm morphology was retained at elevated temperature. (b) ^{1}H NMR spectra recorded at various temperatures for a 5.0% w/w dispersion of the same BIEE cross-linked $PDMS_{66}$-$PDMA_{100}$ worms in D5. A coaxial inner tube containing toluene-d_8 as a lock solvent and pyridine as an external standard was used in this experiment.

Next, a 5.0% w/w dispersion of the BIEE cross-linked $PDMS_{66}$-$PDMA_{100}$ worms in D5 was monitored by variable temperature ^{1}H NMR spectroscopy on heating from 20 to 100 °C

(**Figure 4b**). No PDMA core block signals were observed, even at 100 °C. Thus, the cross-linked worm cores remain non-solvated (unplasticized) at elevated temperatures, suggesting that the degree of core cross-linking is relatively high. Moreover, as cross-linking proceeds and quaternary amine groups are formed, there is a gradual build-up of cationic charge density within the worm cores. Even if the quaternary amine groups and the iodide counter-ions form ion pairs, the rather low relative permittivity of D5 ($\varepsilon \sim 3$)[66] means that this silicone fluid is a very poor solvent for such cationic worm cores. In this context, it is possible that the degree of cross-linking may not be particularly high, but the D5 solvent becomes such a poor solvent for the cationic worm cores after BIEE treatment that surface plasticization can no longer occur.

Variable temperature DLS was used to monitor the behavior of a 0.25% w/w dispersion of linear $PDMS_{66}$-$PDMA_{100}$ worms (**Figure 5a**), and also the corresponding BIEE cross-linked worms (**Figure 5b**) on heating up to 90 °C in D5. The interpretation of DLS data normally relies on the Stokes-Einstein equation, which assumes a spherical morphology.[67] Thus, in these experiments DLS merely reports a sphere-equivalent particle diameter that does not correspond to either the worm length or the worm width. Nevertheless, DLS is still sensitive to a relative change in dimensions and hence can be used to monitor worm-to-sphere transitions.[58,67] The linear worms exhibit an apparent Z-average diameter of 480 ± 280 nm at 20 °C. As this dilute dispersion is heated up to 90 °C, the apparent diameter is progressively reduced to 37 ± 11 nm, which is consistent with the anticipated worm-to-sphere transition (see **Figure 2**). However, the Z-average diameter remains approximately 40 nm on returning to 20 °C, indicating that the original worms are not reformed, at least within the time scale of this experiment (140 min). The formation of such kinetically-trapped spheres is consistent with earlier studies, which indicate that the worm-to-sphere transition is usually irreversible

for sufficiently dilute dispersions of methacrylic diblock copolymer worms in non-polar media.[58]

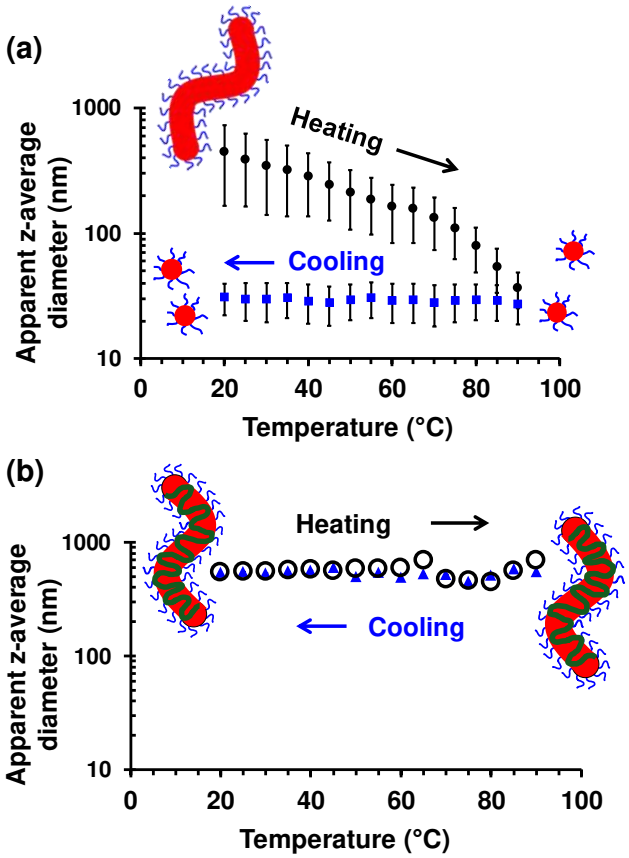

Figure 5. (a) Variable temperature DLS studies of a 0.25 % w/w dispersion of linear $PDMS_{66}$-$PDMA_{100}$ worms subjected to a 20 °C – 90 °C – 20 °C thermal cycle. In this case, heating induces a worm-to-sphere transition but the corresponding sphere-to-worm transition does not occur on cooling, resulting in kinetically-trapped spheres. (b) Variable temperature DLS studies of a dispersion of cross-linked $PDMS_{66}$-$PDMA_{100}$ worms (prepared using a BIEE/DMA molar ratio of 0.15) subjected to a 20 °C – 90 °C – 20 °C thermal cycle. The open black circles were obtained during heating while the filled blue triangles were obtained during cooling. These worms were prepared at 25% w/w before being diluted to 0.25% w/w for core crosslinking. The apparent Z-average diameter remains approximately constant in this case, which confirms that the BIEE cross-linked worms do not possess the thermoresponsive behavior exhibited by the linear precursor worms. For both data sets, inset schematic cartoons indicate the copolymer morphology at 20 °C and 90 °C; error bars represent one standard deviation of the apparent Z-average diameter.

These observations can be explained as follows. The worm-to-sphere transition involves a concentration-independent dissociative mechanism. In contrast, the sphere-to-worm transition is highly cooperative, since worm formation involves the 1D fusion of multiple spheres. The latter process is strongly concentration-dependent, so thermoreversible behavior can be observed at relatively high copolymer concentrations (e.g. 20 % w/w) whereas essentially irreversible behavior is obtained at the relatively low copolymer concentrations required for DLS studies. Similar DLS studies were performed on a 0.25 % w/w dispersion of cross-linked $PDMS_{66}$-$PDMA_{100}$ worms prepared using 15 mol % BIEE relative to the DMA residues. At 20 °C, the cross-linked worms had an apparent Z-average diameter of 540 nm ± 380 nm. This is somewhat larger than that observed for the linear worms, which suggests greater worm stiffness and hence a longer persistence length (see later).[62] Moreover, in this case the apparent Z-average diameter remained roughly constant on heating to 90 °C and returning to 20 °C. This was expected, as the core cross-linked worms are covalently stabilized and hence can no longer undergo a worm-to-sphere transition.

To examine the physical properties of cross-linked $PDMS_{66}$-$PDMA_{100}$ worm gels prepared using varying amounts of BIEE, temperature-dependent oscillatory rheology experiments were conducted. First, analysis of linear $PDMS_{66}$-$PDMA_{100}$ worms at 20 °C yielded G' and G'' values of 94 Pa and 64 Pa, respectively (**Figure 6**), which is consistent with the formation of a free-standing gel. However, G' falls below G'' on heating to 32 °C. This indicates degelation at this temperature, which corresponds to the critical gelation temperature (CGT). The dispersion then remained a free-flowing fluid up to 60°C. On cooling to 20 °C, regelation was observed at 30 °C. This modest shift in the CGT indicates some hysteresis. Such behavior has been previously observed for diblock copolymer worms prepared via PISA.[58] In addition, the G' value obtained at the end of the experiment (68 Pa) was somewhat lower

than that at the start (94 Pa). A plausible explanation for this difference is that the highly cooperative sphere-to-worm transition results in the formation of shorter worms on the time scale of the experiment, which in turn form fewer inter-worm contacts and hence produce weaker gels.[62]

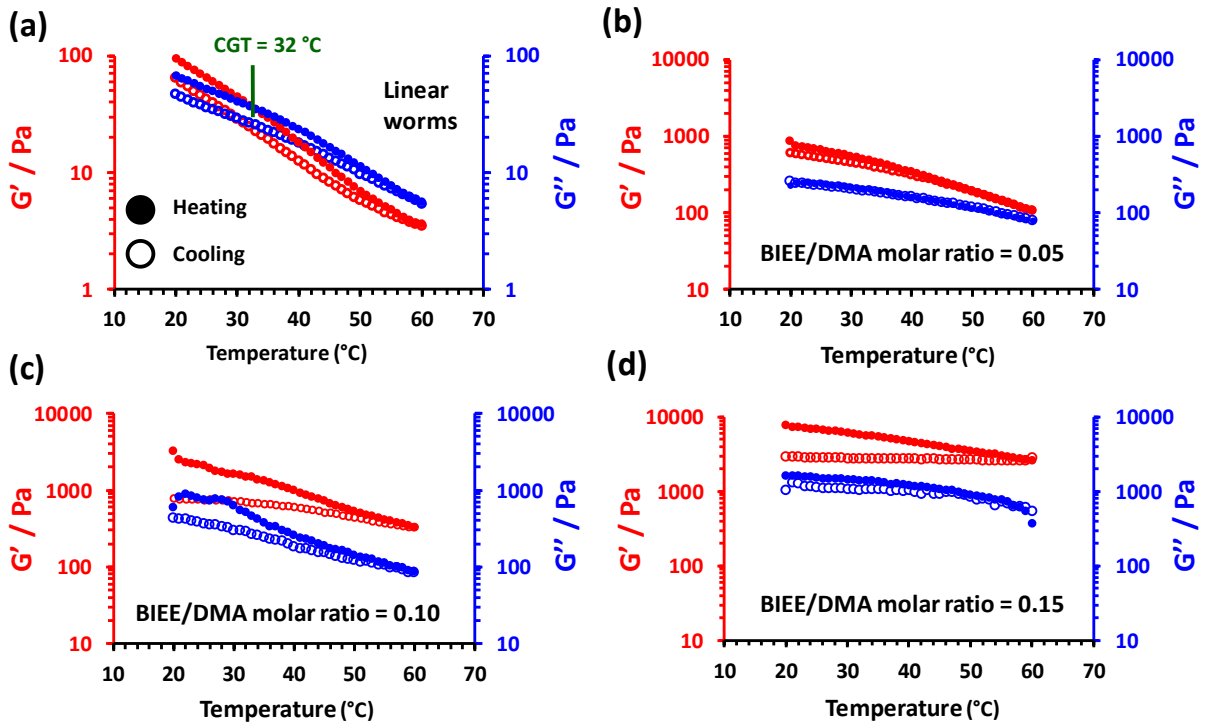

Figure 6. (a) Variable temperature oscillatory rheology measurements performed on 25 % w/w $PDMS_{66}$-$PDMA_{100}$ worms in D5 silicone oil; the point at which G'' exceeds G' defines the critical gelation temperature (CGT), and is indicated in green. Variable temperature oscillatory rheology measurements performed on the same $PDMS_{66}$-$PDMA_{100}$ worms after crosslinking using (b) a BIEE/DMA molar ratio of 0.05, (c) a BIEE/DMA molar ratio of 0.10, (d) a BIEE/DMA molar ratio of 0.15. In all cases, G' data are shown in red while G'' data are shown in blue; filled circles represent heating cycles while open circles represent cooling cycles.

Next, a series of cross-linked $PDMS_{66}$-$PDMA_{100}$ worm gels were prepared using a BIEE/DMA molar ratio ranging between 0.05 and 0.15 and subsequently analyzed *via* oscillatory rheology. Perhaps surprisingly, the addition of only five units of BIEE per $PDMS_{66}$-$PDMA_{100}$ polymer chain (BIEE/DMA = 0.05) was sufficient to suppress degelation.

Moreover, increasing the BIEE concentration produced dramatically stronger gels. For example, a G' of 7855 Pa was observed when using a BIEE/DMA molar ratio of 0.15, which is almost two orders of magnitude greater than that of the original linear worm gel. Interestingly, attempts to cross-link worm gels using a BIEE/DMA molar ratio of 0.20 (or higher) resulted in loss of colloidal stability, causing macroscopic precipitation and concomitant degelation.

Thus far, various techniques have been utilized to characterize the worm-to-sphere transition. However, it is difficult to determine the precise temperature at which all the worms have been fully converted into spheres. For example, TEM is likely to be insensitive to the presence of a minor fraction of worms, which could be easily overlooked. Similarly, copolymer morphologies can only be inferred during DLS studies because a spherical morphology is implicitly assumed for data analysis. To address this issue, shear-induced polarized-light imaging (SIPLI) was utilized.[53] This relatively new technique combines rotational rheology with polarized light imaging to characterize the behavior of materials under shear.[52,53] If anisotropic nanoparticles are subject to shear forces then alignment can occur, which results in birefringence. A material is said to be birefringent if it possesses different indices of refraction, with each index depending on the polarization and direction of propagation of the incident light.[53] If polarized light passes through a birefringent material, rotation of the plane of polarization is observed. In a SIPLI experiment, plane-polarized light is directed through a sample under shear and analyzed at 90 °C to the plane of polarization using a CCD camera.[52,53] As the polarizer and the camera are aligned orthogonally, only rotated light (i.e. that owing to birefringence) is observed. This leads to a characteristic Maltese cross pattern.[68]

First, a 25% w/w dispersion of the linear $PDMS_{66}$-$PDMA_{100}$ worms was analyzed via SIPLI. The viscosity of this dispersion was 4.7 Pa s at 20 °C, which is within the typical range expected for diblock copolymer worms.[68,69] Moreover, a distinct Maltese cross was observed (**Figure 7a**), which indicates the alignment of anisotropic particles under shear. At higher temperatures, the dispersion viscosity is gradually reduced, owing to the formation of a growing population of spheres.

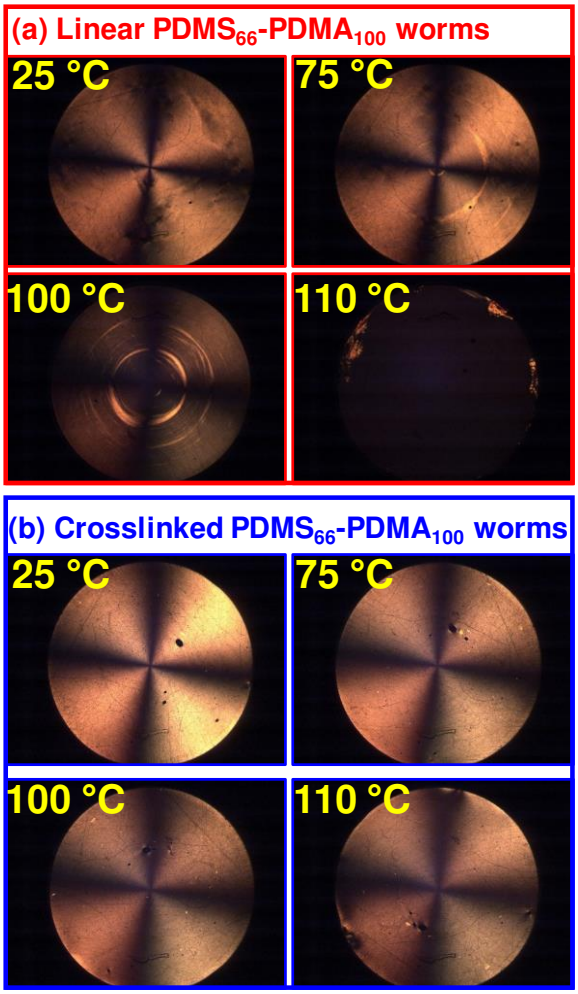

Figure 7: Selected shear-induced polarized light images (SIPLIs) recorded during a temperature ramp from 20 °C to 110 °C for (a) a 25% w/w dispersion of linear $PDMS_{66}$-$PDMA_{100}$ worms in D5 silicone oil and (b) a 25% w/w dispersion of BIEE cross-linked $PDMS_{66}$-$PDMA_{100}$ worms in D5 silicone oil using a BIEE/DMA molar ratio of 0.15. In both cases, the heating rate was 5 °C min^{-1}, the shear rate was 2.0 s^{-1} and the sample gap was 0.5 mm.

However, a Maltese cross is still clearly visible at both 75 °C and 100 °C, indicating that a population of worms is still present. The Maltese cross finally disappears at 110 °C, confirming complete loss of the worm morphology (**Figure 7a**). Furthermore, the viscosity of the dispersion is reduced to 0.3 Pa s at this temperature. This is consistent with that expected for a 25% w/w dispersion of spheres. The TEM images shown in **Figure 2** suggest that 100 °C is sufficient for a complete worm-to-sphere transition. However, TEM is a number-average technique and is therefore insensitive to a relatively small population of worms. In contrast, SIPLI is relatively sensitive to the presence of anisotropic nano-objects. Thus, the minimum temperature required for a complete worm-to-sphere transition is approximately 110 °C. [N.B. Only the heating cycle was performed in this experiment because the volatile nature of the D5 silicone oil led to significant solvent losses at 110 °C, which prevented further imaging]. A similar SIPLI experiment was performed on cross-linked $PDMS_{66}$-$PDMA_{100}$ worms prepared using a BIEE/DMA molar ratio of 0.15 (**Figure 7b**). The dispersion viscosity was 7.18 Pa s at 20 °C, which is significantly higher than that observed for the corresponding linear worms. This is consistent with a longer persistence length, as expected for stiffer worms. Furthermore, on heating up to 110 °C, a Maltese cross remained visible in the polarized light images, confirming the continued presence of covalently-stabilized worms under these conditions.

Both linear and cross-linked $PDMS_{66}$-$PDMA_{100}$ worms were further characterized by synchrotron SAXS experiments performed at ESRF (Grenoble, France). SAXS provides statistically robust structural information, because X-ray scattering is averaged over many millions of nanoparticles. It is well-known that the dominant copolymer morphology can be inferred by inspecting the low q gradient of an $I(q)$ vs. q plot, where q is the scattering vector ($q = 4\pi\sin\theta/\lambda$) and $I(q)$ is the X-ray scattering intensity.[58,70–72] Thus a zero gradient is

expected for spheres, whereas a gradient of -1 is indicative of rods (or worms).[70] First, a 25% w/w dispersion of $PDMS_{66}$-$PDMA_{100}$ worms in D5 was diluted to 1.0% w/w to avoid the presence of a structure factor in the SAXS pattern. This dilute dispersion was then analyzed during a 25 °C – 110 °C – 25 °C thermal cycle and the resulting SAXS patterns are shown in **Figure 8a**.

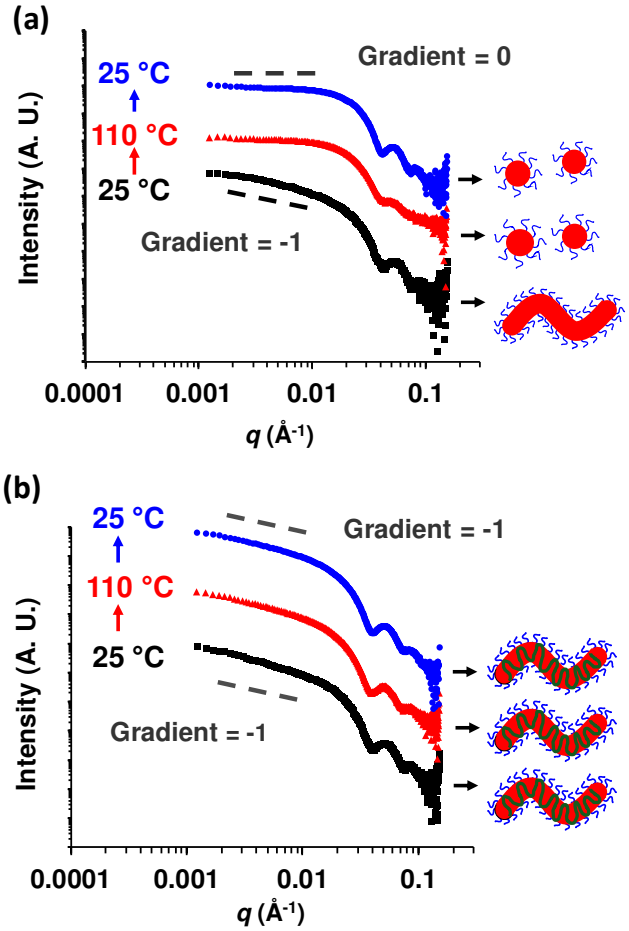

Figure 8. (a) SAXS data obtained for 1.0% w/w dispersions of $PDMS_{66}$-$PDMA_{100}$ worms during a thermal cycle from 25 °C (black trace) to 110 °C (red trace) to 25 °C (blue trace). (b) SAXS data recorded for a 1.0% w/w dispersion of cross-linked $PDMS_{66}$-$PDMA_{100}$ worms prepared using a BIEE/DMA molar ratio of 0.15 during a thermal cycle from 25 °C (black trace) to 110 °C (red trace) to 25 °C (blue trace). Black dashed lines indicating gradients of either 0 or -1 are included as a guide to the eye in each case.

The low *q* gradient is approximately -1 at 25 °C, which indicates the presence of worms. This gradient shifts to zero at 110 °C, indicating the formation of spheres at this temperature. This observation is fully consistent with the SIPLI studies reported above. On returning to 25 °C, the low *q* gradient remains zero, which indicates that the original worms are not reformed. In view of the DLS data discussed above, this observation of kinetically-trapped spheres is not unexpected given that the SAXS experiments are conducted at 1.0% w/w. The corresponding cross-linked $PDMS_{66}$-$PDMA_{100}$ worms prepared using a BIEE/DMA molar ratio of 0.15 were also characterized by SAXS (**Figure 8b**). As expected, a low *q* gradient of -1 was observed in the SAXS pattern recorded at 25 °C. In this case, the SAXS pattern recorded at 110 °C remained essentially unchanged, confirming that the cross-linked worms remain intact at this temperature. This is fully consistent with the TEM, DLS and SIPLI observations, which indicate that such covalently-stabilized $PDMS_{66}$-$PDMA_{100}$ worms cannot undergo a worm-to-sphere transition. The overlaid SAXS traces recorded before and after heating are shown for both the linear and cross-linked worms in **Figure S2**.

According to the literature, core cross-linking of diblock copolymer worms prepared via traditional post-polymerization processing can have a profound effect on their physical properties. For example, Bates and co-workers reported that cross-linked PEO-PB worms are significantly stiffer than their linear analogues.[37] Moreover, such covalently-stabilized worms exhibit a G' value up to two orders of magnitude greater than that of the corresponding linear worms. Similarly, Lovett and co-workers reported that worm stiffness influences the CGC,[62] which is not unexpected in the context of recent developments in percolation theory.[73,74] Thus, the effect of core cross-linking on the CGC of $PDMS_{66}$-$PDMA_{100}$ worms was investigated. Recently, we reported that the CGC of linear $PDMS_{66}$-$PDMA_{100}$ worms lies between 10 and 12.5% w/w, as judged by oscillatory rheology studies conducted at an

angular frequency of 1 rad s^{-1} and an applied strain of 1%.[48] These precise conditions were selected because they fall within the linear viscoelastic region for these worms. To investigate the influence of covalent stabilization on the CGC, a large-scale batch of $PDMS_{66}$-$PDMA_{100}$ worms was prepared at 25% w/w. Portions of this gel were then diluted with D5 to produce copolymer concentrations ranging from 1 to 8% w/w. As expected, each of these worm dispersions formed a free-flowing liquid, as such copolymer concentrations lie below the CGC. This liquid-like character was confirmed by oscillatory rheology studies, which indicated that G'' was greater than G' for each dispersion (when analyzed at an applied strain of 1% and an angular frequency of 1 rad s^{-1}, see **Figure 9a**).

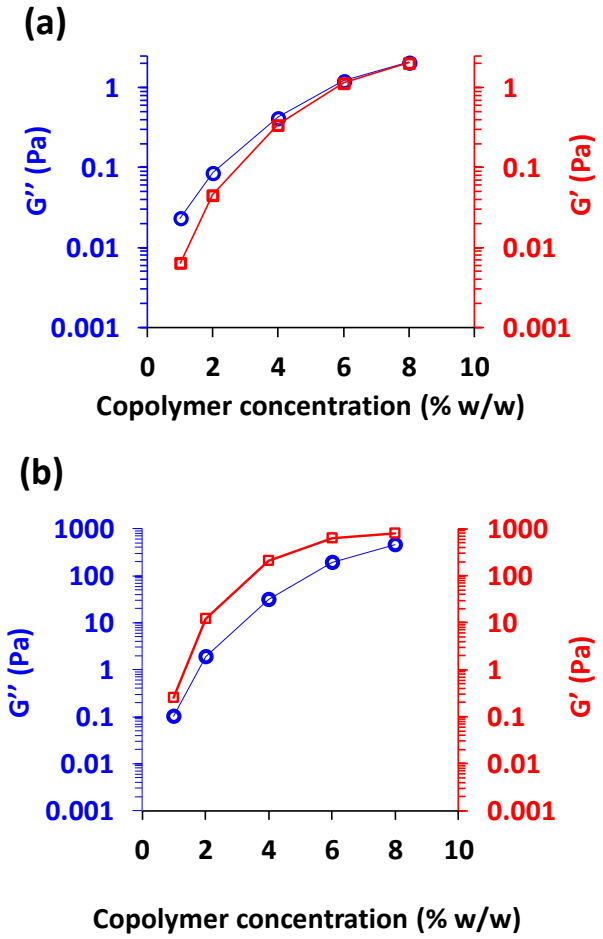

Figure 9. G' (open red squares) and G'' (open blue circles) data determined by oscillatory rheology at an angular frequency of 1 rad s^{-1} and a fixed applied strain of 1% for: (a) a series

of linear $PDMS_{66}$-$PDMA_{100}$ worms at copolymer concentrations ranging from 1 to 8% w/w in D5; (b) a series of BIEE cross-linked $PDMS_{66}$-$PDMA_{100}$ dispersions prepared in D5 using a BIEE/DMA molar ratio of 0.15 over the same range of copolymer concentration.

Next, BIEE was added to the same $PDMS_{66}$-$PDMA_{100}$ worm dispersions using a BIEE/DMA molar ratio of 0.15. Quaternization was allowed to proceed for five days at 20 °C, and the resulting core cross-linked worms were then reanalyzed by oscillatory rheology under identical conditions, i.e. an applied strain of 1% and an angular frequency of 1 rad s^{-1}. Inspecting **Figure 9b,** G' exceeds G'' for a copolymer concentration of 2% w/w or higher. In addition, G' is almost independent of angular frequency (see **Figure S3**), confirming the solid-like nature of these dispersions. Moreover, G' also exceeds G'' at 1% w/w copolymer concentration but the former parameter has a significant frequency dependence under these conditions (see **Figure S3**), suggesting that this dispersion is not a true gel. Nevertheless, it is clear that these cross-linked worms exhibit a significantly lower CGC (~2% w/w) compared to the precursor linear worms (~12% w/w). This is because core crosslinking produces much stiffer worms with a greater mean persistence length and hence a correspondingly lower percolation threshold.[62] The dispersions shown in **Figure 9** were also subjected to the tube inversion test, both before and after cross-linking (see **Figure S4**). Prior to cross-linking, each dispersion is clearly a free-flowing liquid. After crosslinking, $PDMS_{66}$-$PDMA_{100}$ dispersions prepared using more than 4% w/w copolymer concentration form free-standing gels. Below this threshold concentration, rheological studies indicated the formation of gels that were not sufficiently strong enough to remain free-standing after tube inversion.

Finally, in order to estimate the minimum time required for core cross-linking to preserve the worm morphology, a kinetic study was performed on $PDMS_{66}$-$PDMA_{176}$ *vesicles* using ^1H NMR spectroscopy. Vesicles were selected instead of worms for this experiment because (i) their free-flowing nature facilitated rapid mixing with the BIEE reagent and (ii) this fluidity

also greatly aided the periodic sampling required for ^{1}H NMR studies. Thus, sufficient BIEE was added directly to a 25% w/w dispersion of $PDMS_{66}$-$PDMA_{176}$ vesicles in D5 to target a BIEE/DMA molar ratio of 0.15. Aliquots (~0.20 mL) were removed from the reaction mixture after regular time intervals and immediately diluted to 2.5% w/w using chloroform, which is a good solvent for both the $PDMS_{66}$ and $PDMA_{176}$ blocks. Prior to the onset of BIEE cross-linking, such addition of chloroform caused molecular dissolution of the $PDMS_{66}$-$PDMA_{176}$ vesicles to afford copolymer chains. For example, the oxymethylene signal assigned to the $PDMA_{176}$ block was observed at 4.15 ppm in the ^{1}H NMR spectrum (see signal *a* in **Figure 10a**; fully assigned NMR spectra are shown in the Supporting Information, see **Figure S5)**. However, the vesicular morphology became more resistant to dissolution in chloroform as quaternization proceeded. The integrated signals at 2.65 ppm and 4.15 ppm assigned to the PDMA core-forming block and also the BIEE signals at 3.3–3.9 ppm (labeled *a* and *e* and *b-d* respectively in **Figure 10a**), are shown as a function of reaction time in **Figure 10b**, with each signal being normalized relative to an external standard (pyridine). Progressive attenuation of the azamethylene and oxymethylene signals assigned to the PDMA block (at 2.65 ppm and 4.15 ppm respectively) occurred over 13 h at 20 °C. Gradual loss of the BIEE signals was also discernible as this reagent became covalently bound within the vesicle membrane. Once the BIEE has reacted with at least one DMA residue, this reagent can no longer be detected by ^{1}H NMR. However, the *complete* disappearance of the signals assigned to soluble (as yet unreacted) BIEE from the ^{1}H NMR spectrum required a relatively long reaction time (~36 h). TEM images recorded for the linear $PDMS_{66}$-$PDMA_{176}$ vesicles dispersed in D5, the same copolymer dissolved in chloroform and the corresponding BIEE cross-linked vesicles (dispersed in both D5 and chloroform) are shown in **Figure S6**.

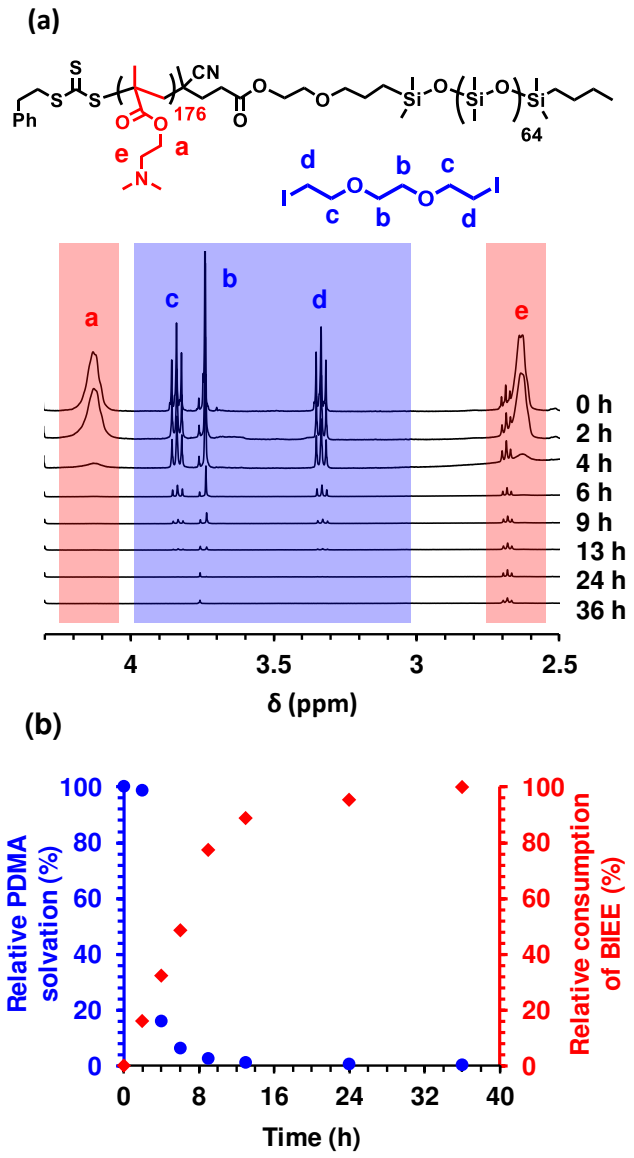

Figure 10. (a) ^{1}H NMR spectra recorded after various intervals at 20 °C for the cross-linking of $PDMS_{66}$-$PDMA_{176}$ vesicles using BIEE at a BIEE/DMA molar ratio of 0.15. This quaternization reaction was performed at 25% w/w in D5 silicone oil and dispersions were diluted to 2.5% w/w in chloroform for ^{1}H NMR analysis. The gradual disappearance of signals *a* and *e* assigned to the PDMA block at 4.15 ppm and 2.65 ppm respectively, and also the BIEE signals at 3.3-3.9 ppm indicates the onset of cross-linking. (b) Kinetics of BIEE cross-linking $PDMS_{66}$-$PDMA_{176}$ vesicles. The degree of solvation of the PDMA block was determined using its oxymethylene signal *a* at 4.15 ppm. The extent of BIEE consumption was monitored using signals *b*, *c* and *d*. All signals were normalized relative to a suitable external standard (0.1 M pyridine in toluene-d_8) contained within a coaxial inner tube.

Conclusions

In summary, linear $PDMS_{66}$-$PDMA_{100}$ worms prepared at 25% w/w in D5 silicone oil exhibit a thermoreversible worm-to-sphere transition on heating to 100 °C. Variable temperature ^{1}H NMR studies suggest that this behavior is the result of surface plasticization of the core-forming PDMA block. This worm-to-sphere transition was also monitored by variable temperature DLS, SAXS and SIPLI. These techniques indicated that, although degelation occurs at just 32 °C, heating up to 110 °C is required for the complete conversion of worms into spheres.

Addition of a bifunctional reagent, BIEE, leads to cross-linking of the PDMA worm cores via quaternization. The crosslinked $PDMS_{66}$-$PDMA_{100}$ worms no longer exhibit a worm-to-sphere transition at 110 °C, with this highly anisotropic morphology remaining intact at this temperature. Furthermore, ^{1}H NMR spectroscopy studies indicated no detectable solvation of the partially quaternized core-forming block even at 100 °C. This either indicates extensive cross-linking and/or simply reflects the fact that D5 is a much poorer solvent for the partially quaternized PDMA chains than for the original neutral PDMA chains. Interestingly, cross-linked $PDMS_{66}$-$PDMA_{100}$ worms exhibit a CGC of approximately 2.0% w/w, which is significantly lower than the CGC of 10–12.5% w/w obtained for the corresponding linear worms. Moreover, addition of BIEE to a 25% w/w dispersion of $PDMS_{66}$-$PDMA_{100}$ worms (BIEE/DMA molar ratio = 0.15) resulted in an increase in gel strength (G') from 94 Pa to 7855 Pa. This is the result of core cross-linking, which leads to much stiffer worms. Finally, ^{1}H NMR spectroscopy was used to monitor the kinetics of BIEE cross-linking for a 25% w/w dispersion of $PDMS_{66}$-$PDMA_{176}$ vesicles using a BIEE/DMA molar ratio of 0.15. Within approximately 6 h, the resulting covalently-stabilized vesicles become sufficiently robust to withstand dissolution when diluted using chloroform, which is a good solvent for both

blocks. However, a reaction time of 36 h is required for all of the BIEE molecules to react *at least once* at 20 °C.

Declaration

The authors declare no competing financial interest.

ORCID

Steven P. Armes: 0000-0002-8289-6351

Matthew J. Rymaruk: 0000-0002-6622-6251

Acknowledgments

We thank EPSRC for a CDT PhD studentship for M.J.R. (EP/ L016281) and the Scott Bader Company Ltd. for CASE support of this project and for permission to publish these results. S.P.A. acknowledges an EPSRC Particle Technology Fellowship grant (EP/R003009). The authors thank Christopher Hill and Dr. Svetomir Tzokov at the University of Sheffield Biomedical Science Electron Microscopy suite. We gratefully acknowledge the European Synchrotron Radiation Facility at the ID02 beamline (ESRF, SC-4864) for providing beam time.

Summary of supporting information.

The Supporting information is available free of charge on the ACS publications website at DOI:

Table of copolymer characterization data, additional ^{1}H NMR spectra, overlaid SAXS patterns of $PDMS_{66}$-$PDMA_{100}$ worms before and after heating, digital photographs recorded

for linear and cross-linked worm gels (tube inversion test), oscillatory rheology frequency sweeps and further TEM images.

References

(1) Derry, M. J.; Fielding, L. A.; Armes, S. P. Polymerization-Induced Self-Assembly of Block Copolymer Nanoparticles via RAFT Non-Aqueous Dispersion Polymerization. *Prog. Polym. Sci.* **2016**, *52*, 1–18.

(2) Canning, S. L.; Smith, G. N.; Armes, S. P. A Critical Appraisal of RAFT-Mediated Polymerization-Induced Self-Assembly. *Macromolecules* **2016**, *49*, 1985–2001.

(3) Warren, N. J.; Armes, S. P. Polymerization-Induced Self-Assembly of Block Copolymer Nano-Objects via RAFT Aqueous Dispersion Polymerization. *J. Am. Chem. Soc.* **2014**, *136*, 10174–10185.

(4) Charleux, B.; Delaittre, G.; Rieger, J.; D'Agosto, F. Polymerization-Induced Self-Assembly: From Soluble Macromolecules to Block Copolymer Nano-Objects in One Step. *Macromolecules* **2012**, *45*, 6753–6765.

(5) Mai, Y.; Eisenberg, A. Self-Assembly of Block Copolymers. *Chem. Soc. Rev.* **2012**, *41*, 5969–5985.

(6) Blanazs, A.; Ryan, A. J.; Armes, S. P. Predictive Phase Diagrams for RAFT Aqueous Dispersion Polymerization: Effect of Block Copolymer Composition, Molecular Weight, and Copolymer Concentration. *Macromolecules* **2012**, *45*, 5099–5107.

(7) Sugihara, S.; Blanazs, A.; Armes, S. P.; Ryan, A. J.; Lewis, A. L. Aqueous Dispersion Polymerization: A New Paradigm for in Situ Block Copolymer Self-Assembly in Concentrated Solution. *J. Am. Chem. Soc.* **2011**, *133*, 15707–15713.

(8) Mable, C. J.; Gibson, R. R.; Prevost, S.; McKenzie, B. E.; Mykhaylyk, O. O.; Armes, S. P. Loading of Silica Nanoparticles in Block Copolymer Vesicles during

Polymerization-Induced Self-Assembly: Encapsulation Efficiency and Thermally Triggered Release. *J. Am. Chem. Soc.* **2015**, *137*, 16098–16108.

(9) Canton, I.; Warren, N. J.; Chahal, A.; Amps, K.; Wood, A.; Weightman, R.; Wang, E.; Moore, H.; Armes, S. P. Mucin-Inspired Thermoresponsive Synthetic Hydrogels Induce Stasis in Human Pluripotent Stem Cells and Human Embryos. *ACS Cent. Sci.* **2016**, *2*, 65–74.

(10) Mable, C. J.; Canton, I.; Mykhaylyk, O. O.; Ustbas Gul, B.; Chambon, P.; Themistou, E.; Armes, S. P. Targeting Triple-Negative Breast Cancer Cells Using Dengue Virus-Mimicking pH-Responsive Framboidal Triblock Copolymer Vesicles. *Chem. Sci.* **2019**, *10*, 4811–4821.

(11) Rymaruk, M. J.; Thompson, K. L.; Derry, M. J.; Warren, N. J.; Ratcliffe, L. P. D.; Williams, C. N.; Brown, S. L.; Armes, S. P. Bespoke Contrast-Matched Diblock Copolymer Nanoparticles Enable the Rational Design of Highly Transparent Pickering Double Emulsions. *Nanoscale* **2016**, *8*, 14497–14506.

(12) Thompson, K. L.; Mable, C. J.; Cockram, A.; Warren, N. J.; Cunningham, V. J.; Jones, E. R.; Verber, R.; Armes, S. P. Are Block Copolymer Worms More Effective Pickering Emulsifiers than Block Copolymer Spheres? *Soft Matter* **2014**, *10*, 8615–8626.

(13) Thompson, K. L.; Chambon, P.; Verber, R.; Armes, S. P. Can Polymersomes Form Colloidosomes? *J. Am. Chem. Soc.* **2012**, *134*, 12450–12453.

(14) Thompson, K. L.; Fielding, L. A.; Mykhaylyk, O. O.; Lane, J. A.; Derry, M. J.; Armes, S. P. Vermicious Thermo-Responsive Pickering Emulsifiers. *Chem. Sci.* **2015**, *6*, 4207–4214.

(15) Mable, C. J.; Warren, N. J.; Thompson, K. L.; Mykhaylyk, O. O.; Armes, S. P. Framboidal ABC Triblock Copolymer Vesicles: A New Class of Efficient Pickering

Emulsifier. *Chem. Sci.* **2015**, *6*, 6179–6188.

(16) Mable, C. J.; Thompson, K. L.; Derry, M. J.; Mykhaylyk, O. O.; Binks, B. P.; Armes, S. P. ABC Triblock Copolymer Worms: Synthesis, Characterization, and Evaluation as Pickering Emulsifiers for Millimeter-Sized Droplets. *Macromolecules* **2016**, *49*, 7897–7907.

(17) O'Reilly, R. K.; Hawker, C. J.; Wooley, K. L. Cross-Linked Block Copolymer Micelles: Functional Nanostructures of Great Potential and Versatility. *Chem. Soc. Rev.* **2006**, *35*, 1068–1083.

(18) Read, E. S.; Armes, S. P. Recent Advances in Shell Cross-Linked Micelles. *Chem. Commun.* **2007**, No. 29, 3021–3035.

(19) Thurmond, K. B.; Kowalewski, T.; Wooley, K. L. Water-Soluble Knedel-like Structures: The Preparation of Shell-Cross-Linked Small Particles. *J. Am. Chem. Soc.* **1996**, *118*, 7239–7240.

(20) Thurmond, K. B.; Huang, H.; Clark, C. G.; Kowalewski, T.; Wooley, K. L. Shell Cross-Linked Polymer Micelles: Stabilized Assemblies with Great Versatility and Potential. *Colloids Surfaces B Biointerfaces* **1999**, *16*, 45–54.

(21) Joralemon, M. J.; O'Reilly, R. K.; Hawker, C. J.; Wooley, K. L. Shell Click-Crosslinked (SCC) Nanoparticles: A New Methodology for Synthesis and Orthogonal Functionalization. *J. Am. Chem. Soc.* **2005**, *127*, 16892–16899.

(22) Ding, J.; Liu, G. Polystyrene- B Lock -poly(2-Cinnamoylethyl Methacrylate) Nanospheres with Cross-Linked Shells. *Macromolecules* **1998**, *31*, 6554–6558.

(23) Weaver, J. V. M.; Tang, Y.; Liu, S.; Iddon, P. D.; Grigg, R.; Billingham, N. C.; Armes, S. P.; Hunter, R.; Rannard, S. P. Preparation of Shell Cross-Linked Micelles by Polyelectrolyte Complexation. *Angew. Chemie - Int. Ed.* **2004**, *43*, 1389–1392.

(24) Fujii, S.; Cai, Y.; Weaver, J. V. M.; Armes, S. P. Syntheses of Shell Cross-Linked

Micelles Using Acidic ABC Triblock Copolymers and Their Application as pH-Responsive Particulate Emulsifiers. *J. Am. Chem. Soc.* **2005**, *127*, 7304–7305.

(25) Lokitz, B. S.; Convertine, A. J.; Ezell, R. G.; Heidenreich, A.; Li, Y.; McCormick, C. L. Responsive Nanoassemblies via Interpolyelectrolyte Complexation of Amphiphilic Block Copolymer Micelles. *Macromolecules* **2006**, *39*, 8594–8602.

(26) Bütün, V.; Billingham, N. C.; Armes, S. P. Synthesis of Shell Cross-Linked Micelles with Tunable Hydrophilic/Hydrophobic Cores. *J. Am. Chem. Soc.* **1998**, *120*, 12135–12136.

(27) Bütün, V.; Wang, X. S.; De Paz Báñez, M. V.; Robinson, K. L.; Billingham, N. C.; Armes, S. P.; Tuzar, Z. Synthesis of Shell Cross-Linked Micelles at High Solids in Aqueous Media. *Macromolecules* **2000**, *33*, 1–3.

(28) Bütün, V.; Top, R. B.; Ufuklar, S. Synthesis and Characterization of Novel "Schizophrenic" Water-Soluble Triblock Copolymers and Shell Cross-Linked Micelles. *Macromolecules* **2006**, *39*, 1216–1225.

(29) Bütün, V.; Lowe, A. B.; Billingham, N. C.; Armes, S. P. Synthesis of Zwitterionic Shell Cross-Linked Micelles. *J. Am. Chem. Soc.* **1999**, *121*, 4288–4289.

(30) Huang, H.; Kowalewski, T.; Remsen, E. E.; Gertzmann, R.; Wooley, K. L. Hydrogel-Coated Glassy Nanospheres: A Novel Method for the Synthesis of Shell Cross-Linked Knedels. *J. Am. Chem. Soc.* **1997**, *119*, 11653–11659.

(31) Thurmond, K. B.; Kowalewski, T.; Wooley, K. L. Shell Cross-Linked Knedels: A Synthetic Study of the Factors Affecting the Dimensions and Properties of Amphiphilic Core-Shell Nanospheres. *J. Am. Chem. Soc.* **1997**, *119*, 6656–6665.

(32) Guo, A.; Liu, G.; Tao, J. Star Polymers and Nanospheres from Cross-Linkable Diblock Copolymers. *Macromolecules* **1996**, *29*, 2487–2493.

(33) Henselwood, F.; Liu, G. Water-Soluble Porous Nanospheres. *Macromolecules* **1998**,

31, 4213–4217.

(34) Henselwood, F.; Liu, G. Water-Soluble Nanospheres of Poly(2-Cinnamoylethyl Methacrylate)- Block -Poly(acrylic Acid). *Macromolecules* **1997**, *30*, 488–493.

(35) Procházka, K.; Baloch, M. K.; Tuzar, Z. Photochemical Stabilization of Block Copolymer Micelles. *Die Makromol. Chemie* **1979**, *180*, 2521–2523.

(36) Hentze, H.-P.; Krämer, E.; Berton, B.; Förster, S.; Antonietti, M.; Dreja, M. Lyotropic Mesophases of Poly(ethylene Oxide)- B -Poly(butadiene) Diblock Copolymers and Their Cross-Linking To Generate Ordered Gels. *Macromolecules* **1999**, *32*, 5803–5809.

(37) Won, Y.-Y.; Davis, H. T.; Bates, F. S. Giant Wormlike Rubber Micelles. *Science* **1999**, *283*, 960–963.

(38) Li, Y.; Armes, S. P. RAFT Synthesis of Sterically Stabilized Methacrylic Nanolatexes and Vesicles by Aqueous Dispersion Polymerization. *Angew. Chem. Int. Ed. Engl.* **2010**, *49*, 4042–4046.

(39) Liu, G.; Qiu, Q.; Shen, W.; An, Z. Aqueous Dispersion Polymerization of 2-Methoxyethyl Acrylate for the Synthesis of Biocompatible Nanoparticles Using a Hydrophilic RAFT Polymer and a Redox Initiator. *Macromolecules* **2011**, *44*, 5237–5245.

(40) Liu, G.; Qiu, Q.; An, Z. Development of Thermosensitive Copolymers of poly(2-Methoxyethyl Acrylate-Co-Poly(ethylene Glycol) Methyl Ether Acrylate) and Their Nanogels Synthesized by RAFT Dispersion Polymerization in Water. *Polym. Chem.* **2012**, *3*, 504–513.

(41) Lovett, J. R.; Ratcliffe, L. P. D.; Warren, N. J.; Armes, S. P.; Smallridge, M. J.; Cracknell, R. B.; Saunders, B. R. A Robust Cross-Linking Strategy for Block Copolymer Worms Prepared via Polymerization-Induced Self-Assembly.

Macromolecules **2016**, *49*, 2928–2941.

(42) Liu, G.; Qiao, L.; Guo, A. Diblock Copolymer Nanofibers. *Macromolecules* **1996**, *29*, 5508–5510.

(43) Penfold, N. J. W.; Ning, Y.; Verstraete, P.; Smets, J.; Armes, S. P. Cross-Linked Cationic Diblock Copolymer Worms Are Superflocculants for Micrometer-Sized Silica Particles. *Chem. Sci.* **2016**, *7*, 6894–6904.

(44) Byard, S. J.; Williams, M.; McKenzie, B. E.; Blanazs, A.; Armes, S. P. Preparation and Cross-Linking of All-Acrylamide Diblock Copolymer Nano-Objects via Polymerization-Induced Self-Assembly in Aqueous Solution. *Macromolecules* **2017**, *50*, 1482–1493.

(45) Kessel, N.; Illsley, D. R.; Keddie, J. L. The Diacetone Acrylamide Crosslinking Reaction and Its Influence on the Film Formation of an Acrylic Latex. *J. Coatings Technol. Res.* **2008**, *5*, 285–297.

(46) Hatton, F. L.; Lovett, J. R.; Armes, S. P. Synthesis of Well-Defined Epoxy-Functional Spherical Nanoparticles by RAFT Aqueous Emulsion Polymerization. *Polym. Chem.* **2017**, *8*, 4856–4868.

(47) Docherty, P. J.; Derry, M. J.; Armes, S. P. RAFT Dispersion Polymerization of Glycidyl Methacrylate for the Synthesis of Epoxy-Functional Block Copolymer Nanoparticles in Mineral Oil. *Polym. Chem.* **2019**, *10*, 603–611.

(48) Rymaruk, M. J.; Hunter, S. J.; O'Brien, C. T.; Brown, S. L.; Williams, C. N.; Armes, S. P. RAFT Dispersion Polymerization in Silicone Oil. *Macromolecules* **2019**, *52*, 2822–2832.

(49) Mable, C. J.; Fielding, L. A.; Derry, M. J.; Mykhaylyk, O. O.; Chambon, P.; Armes, S. P. Synthesis and pH-Responsive Dissociation of Framboidal ABC Triblock Copolymer Vesicles in Aqueous Solution. *Chem. Sci.* **2018**, *9*, 1454–1463.

(50) Sola, M.; Lledos, A.; Duran, M.; Bertran, J.; Abboud, J. L. M. Analysis of Solvent Effects on the Menshutkin Reaction. *J. Am. Chem. Soc.* **1991**, *113*, 2873–2879.

(51) Trent, J. S.; Scheinbeim, J. I.; Couchman, P. R. Ruthenium Tetraoxide Staining of Polymers for Electron Microscopy. *Macromolecules* **1983**, *16*, 589–598.

(52) Mykhaylyk, O. O. Time-Resolved Polarized Light Imaging of Sheared Materials: Application to Polymer Crystallization. *Soft Matter* **2010**, *6*, 4430–4440.

(53) Mykhaylyk, O. O.; Warren, N. J.; Parnell, A. J.; Pfeifer, G.; Laeuger, J. Applications of Shear-Induced Polarized Light Imaging (SIPLI) Technique for Mechano-Optical Rheology of Polymers and Soft Matter Materials. *J. Polym. Sci. Part B Polym. Phys.* **2016**, *54*, 2151–2170.

(54) Pei, Y.; Sugita, O. R.; Thurairajah, L.; Lowe, A. B. Synthesis of Poly(stearyl Methacrylate-B-3-Phenylpropyl Methacrylate) Nanoparticles in N-Octane and Associated Thermoreversible Polymorphism. *RSC Adv.* **2015**, *5*, 17636–17646.

(55) Pei, Y.; Thurairajah, L.; Sugita, O. R.; Lowe, A. B. RAFT Dispersion Polymerization in Nonpolar Media: Polymerization of 3-Phenylpropyl Methacrylate in N -Tetradecane with Poly(stearyl Methacrylate) Homopolymers as Macro Chain Transfer Agents. *Macromolecules* **2015**, *48*, 236–244.

(56) Wang, X.; Zhou, J.; Lv, X.; Zhang, B.; An, Z. Temperature-Induced Morphological Transitions of Poly(dimethylacrylamide)–Poly(diacetone Acrylamide) Block Copolymer Lamellae Synthesized via Aqueous Polymerization-Induced Self-Assembly. *Macromolecules* **2017**, *50*, 7222–7232.

(57) Wang, X.; An, Z. New Insights into RAFT Dispersion Polymerization-Induced Self-Assembly: From Monomer Library, Morphological Control, and Stability to Driving Forces. *Macromol. Rapid Commun.* **2019**, *40*, 1800325.

(58) Fielding, L. A.; Lane, J. A.; Derry, M. J.; Mykhaylyk, O. O.; Armes, S. P. Thermo-

Responsive Diblock Copolymer Worm Gels in Non-Polar Solvents. *J. Am. Chem. Soc.* **2014**, *136*, 5790–5798.

(59) Blanazs, A.; Verber, R.; Mykhaylyk, O. O.; Ryan, A. J.; Heath, J. Z.; Douglas, C. W. I.; Armes, S. P. Sterilizable Gels from Thermoresponsive Block Copolymer Worms. *J. Am. Chem. Soc.* **2012**, *134*, 9741–9748.

(60) Derry, M. J.; Mykhaylyk, O. O.; Armes, S. P. A Vesicle-to-Worm Transition Provides a New High-Temperature Oil Thickening Mechanism. *Angew. Chemie - Int. Ed.* **2017**, *129*, 1772–1776.

(61) Warren, N. J.; Armes, S. P. Polymerization-Induced Self-Assembly of Block Copolymer Nano-Objects via RAFT Aqueous Dispersion Polymerization. *J. Am. Chem. Soc.* **2014**, *136*, 10174–10185.

(62) Lovett, J. R.; Derry, M. J.; Yang, P.; Hatton, F. L.; Warren, N. J.; Fowler, P. W.; Armes, S. P. Can Percolation Theory Explain the Gelation Behavior of Diblock Copolymer Worms? *Chem. Sci.* **2018**, *9*, 7138–7144.

(63) Pal, S.; Ghosh Roy, S.; De, P. Synthesis via RAFT Polymerization of Thermo- and pH-Responsive Random Copolymers Containing Cholic Acid Moieties and Their Self-Assembly in Water. *Polym. Chem.* **2014**, *5*, 1275–1284.

(64) Liu, S.; Weaver, J. V. M.; Tang, Y.; Billingham, N. C.; Armes, S. P.; Tribe, K. Synthesis of Shell Cross-Linked Micelles with pH-Responsive Cores Using ABC Triblock Copolymers. *Macromolecules* **2002**, *35*, 6121–6131.

(65) Busatto, N.; Stolojan, V.; Shaw, M.; Keddie, J. L.; Roth, P. J. Reactive Polymorphic Nanoparticles: Preparation via Polymerization-Induced Self-Assembly and Postsynthesis Thiol- Para -Fluoro Core Modification. *Macromol. Rapid Commun.* **2019**, *40*, 1800346.

(66) Mannsfeld, S. C. B.; Tee, B. C. K.; Stoltenberg, R. M.; Chen, C. V. H.-H.; Barman, S.;

Muir, B. V. O.; Sokolov, A. N.; Reese, C.; Bao, Z. Highly Sensitive Flexible Pressure Sensors with Microstructured Rubber Dielectric Layers. *Nat. Mater.* **2010**, *9*, 859–864.

(67) Bhattacharjee, S. DLS and Zeta Potential – What They Are and What They Are Not? *J. Control. Release* **2016**, *235*, 337–351.

(68) Warren, N. J.; Derry, M. J.; Mykhaylyk, O. O.; Lovett, J. R.; Ratcliffe, L. P. D.; Ladmiral, V.; Blanazs, A.; Fielding, L. A.; Armes, S. P. Critical Dependence of Molecular Weight on Thermoresponsive Behavior of Diblock Copolymer Worm Gels in Aqueous Solution. *Macromolecules* **2018**, *51*, 8357–8371.

(69) Lopez-Oliva, A. P.; Warren, N. J.; Rajkumar, A.; Mykhaylyk, O. O.; Derry, M. J.; Doncom, K. E. B.; Rymaruk, M. J.; Armes, S. P. Polydimethylsiloxane-Based Diblock Copolymer Nano-Objects Prepared in Nonpolar Media via RAFT-Mediated Polymerization-Induced Self-Assembly. *Macromolecules* **2015**, *48*, 3547–3555.

(70) Derry, M. J.; Fielding, L. A.; Warren, N. J.; Mable, C. J.; Smith, A. J.; Mykhaylyk, O. O.; Armes, S. P. In Situ Small-Angle X-Ray Scattering Studies of Sterically-Stabilized Diblock Copolymer Nanoparticles Formed during Polymerization-Induced Self-Assembly in Non-Polar Media. *Chem. Sci.* **2016**, *7*, 5078–5090.

(71) Warren, N. J.; Mykhaylyk, O. O.; Mahmood, D.; Ryan, A. J.; Armes, S. P. RAFT Aqueous Dispersion Polymerization Yields Poly(ethylene Glycol)-Based Diblock Copolymer Nano-Objects with Predictable Single Phase Morphologies. *J. Am. Chem. Soc.* **2014**, *136*, 1023–1033.

(72) Schnablegger, H.; Singh, Y. *The SAXS Guide: Getting Aquainted with the Principles*, 2nd ed.; Anton Paar GmbH: Gratz, 2011.

(73) Chatterjee, A. P. Connectedness Percolation in Polydisperse Rod Systems: A Modified Bethe Lattice Approach. *J. Chem. Phys.* **2010**, *132*, 224905.

(74) Otten, R. H. J.; van der Schoot, P. Connectivity Percolation of Polydisperse

Anisotropic Nanofillers. *J. Chem. Phys.* **2011**, *134*, 94902.